International Journal of Heat and Mass Transfer xxx (2009) xxx–xxx

Contents lists available at ScienceDirect

International Journal of Heat and Mass Transfer

journal homepage: www.elsevier.com/locate/ijhmt

Probabilistic flow pattern-based heat transfer correlation for condensing intermittent flow of refrigerants in smooth horizontal tubes

E. van Rooyen, M. Christians, L. Liebenberg, J.P. Meyer *

Department of Mechanical and Aeronautical Engineering, University of Pretoria, Pretoria 0002, South Africa

ARTICLE INFO

Article history:
Received 18 March 2009
Accepted 1 September 2009
Available online xxxx

Keywords:
Condensation
Smooth tube
Flow pattern
Time-fraction
Heat transfer
Time–frequency
Probabilistic

ABSTRACT

This paper presents a signal analysis method used for condensing refrigerants that results in a modification in the prediction method for heat transfer based on probabilistic time-fractional results. Development of an objective visual method for discrimination of flow patterns and determining probabilistic time-fractions in intermittent flow is presented. The frequency domain was identified as the main candidate for discrimination of sub-regimes present in intermittent flow. Experimental work was conducted using refrigerants R-22 and R-134a, at an average saturation temperature of 40 °C, with mass fluxes ranging from 200 to 700 kg/m^2 s, and with test section inlet vapour qualities ranging from 0.65 down to 0.10. These test conditions mostly represent intermittent flow. The new time fraction-corrected flow regime-based heat transfer correlation is heavily based on the Thome et al. (2003) [36] correlation. The modified correlation predicted the experimental data with a mean absolute deviation of 10%.

1. Introduction

Several methods of signal analysis and measurement techniques have been defined in the recent past that investigate flow patterns [1–3]. These methods bring a greater level of objectivity to flow pattern discrimination. The driving force for research in flow patterns is to gain insight into the physical properties governing two-phase flows. Most recent models of heat transfer and pressure drop are based on flow patterns [4,5].

Probabilistic time-fractional data have been presented by Niño et al. [6] for multiport microchannel flow. Statistically, a sample population of images was taken for analysis at a range of mass fluxes and vapour qualities. Analysis of the still images showed that it was possible to simultaneously exhibit different flow regimes. The flow regimes were classified according to the fraction of time that they were likely to be found in the tubes as a function of vapour quality.

Recently, a time-fractional probabilistic flow map for macro-channels [7] was developed. This was done by capturing video images of the entire flow regime map and analysing it with software developed for flow pattern recognition. The flow pattern recognition method is advanced and it transforms each image with a filter after which the compositional flow patterns appear distinctly. The results of the work done by Jassim et al. [7] was a heat transfer, pressure drop and void fraction prediction method based on time-fractions and parameterised in terms of the refrigerant thermophysical properties and flow conditions [8].

Another method used for flow pattern research developed by Revellin et al. [9] involves lasers emitting light through a tube and a light-sensitive diode to pick up the light intensity. This method was used for micro-channels, but can be adapted for macro-scale work. By accurately spacing two measurement points, this method could be used to calculate velocities, bubble coalescence rates and frequency analysis.

An additional method to objectively classify two-phase flow patterns has been developed by Canière et al. [10], which involves using an in-line capacitance sensor to measure the real-time difference in capacitance between the two phases. The sensor developed was satisfactorily tested with demineralized water and air mixtures; they were able to successfully and objectively classify the different flow patterns tested. From these results, they were able to generate a probabilistic flow pattern map based solely on the capacitive measurements, as shown in Canière et al. [11]. It was shown that this sensor and the method developed would be suitable for use with refrigerants, albeit with smaller capacitance differences between the two phases.

Neutron radiography has been used [12,13] to visualise and measure air–water two-phase flows in vertical channels. The neutron radiography method allowed the measurement of bubble velocity, wave height, interfacial area, void profile and average void fraction. Void fraction measurements were averaged at 30 frames per second and compared to the gas velocity prediction with a drift flux void fraction correlation. No mention was made of time fractions.

* Corresponding author. Tel.: +27 (0)12 420 3104; fax: +27 (0)12 362 5124.
E-mail address: josua.meyer@up.ac.za (J.P. Meyer).

0017-9310/$ - see front matter © 2009 Elsevier Ltd. All rights reserved.
doi:10.1016/j.ijheatmasstransfer.2009.12.005

Nomenclature

A	area (m^2)
a_1, a_2	function coefficients
b_1, b_2	function coefficients
d	diameter (m)
EB	energy balance
f_i	interfacial correction factor
G	mass flux ($kg\,m^{-2}\,s^{-1}$)
g	gravitational acceleration (ms^{-2})
h	enthalpy ($J\,kg^{-1}$)
h	heat transfer coefficient ($W\,m^{-2}K^{-1}$)
k	thermal conductivity ($W\,m^{-1}K^{-1}$)
L	length of test section (m)
$\dot{m}$	mass flow rate ($kg\,s^{-1}$)
Pr	Prandtl number ($c_p\ \mu\ k_l^{-1}$)
$\dot{Q}$	heat transferred (W)
r	radius (m)
Re	Reynolds number ($GD\mu_l^{-1}$)
R^2	Coefficient of determination
R_w	wall thermal resistance ($K\,W^{-1}$)
T	temperature (°C)
$\overline{T}$	mean temperature (°C)
tf	time fraction
u	velocity ($m\,s^{-1}$)
x	vapour quality/thermocouple position (m)

Greek symbols

δ	film thickness (m)
ε	void fraction
θ	falling film angle (rad)
μ	viscosity (Pa s)
ρ	density ($kg\,m^{-3}$)
σ	surface tension ($N\,m^{-1}$)

Subscripts

b	bulk
c	convective
$corr$	correlations
Cu	copper
exp	experimental
f	friction/film
$grav$	gravity-dominated
h	Homogeneous
H_2O	water
i	inner/inlet
IA	intermittent-annular transition
j	inlet/outlet of test section
k	position prior to j
L	liquid/length
m	mean
o	outer
ra	Rouhani-Axelsson
ref	refrigerant
sat	saturation
$shear$	shear stress-dominated
$strat$	stratified
tf	time fraction
V	vapour
w	wall
$wavy$	intermittent-wavy transition

The light extinction technique was used by Shamoun et al. [14] to predict void fraction in a stagnant pool. The effects of light extinction become very complicated for tube flows and cannot be measured accurately by this method [15]. The method of Berthold et al. [15] is an elaboration of the Shamoun et al. [14] method in an attempt to take different types of light scattering and flow effects into account for void fraction prediction.

As proven by Hervieu and Seleghim [16], the time–frequency domain analysis of the signal from an inductive sensor can be used as an objective indicator of the flow regime. Later, the use of time–frequency analysis in the intermittent regime to prove the existence of sub-regimes was done by Klein et al. [17]. In these cases, an inductive sensor was used on air–water flows and in both cases, the method proved successful in identifying flow regimes. The use of time–frequency analysis has not been exploited much further.

The basic premise of time–frequency representation is to divide the signal into smaller parts and to analyse each part separately in the frequency domain. A time–frequency distribution is a transform that maps a one-dimensional time-domain signal into a two-dimensional time–frequency map that describes how the frequency content changes with time. Some methods that can be used to obtain a time–frequency spectrum include the short-time Fourier transform, a Wigner-Ville spectrum or wavelet transform [18,19].

1.1. Flow patterns

Numerous flow pattern maps have been proposed over the years for predicting two-phase flow regime transitions in horizontal tubes under adiabatic and diabatic conditions [20,21]. Kattan et al. [22–25] proposed the first flow-boiling model for evaporation inside horizontal tubes based on the local flow pattern and a newly developed diabatic flow pattern map based on a modification of the Taitel and Dukler [26] map, which in turn is a modification of the original Shao and Granryd [27] map. Stemming from the above, several new condensation heat transfer models based on local flow patterns have been proposed by Shao and Granryd [28] and Cavallini et al. [29,30]. El Hajan et al. [31] adapted the flow-boiling two-phase flow pattern map, originally developed by Kattan et al. [24,25] for condensation inside horizontal tubes.

1.2. Heat transfer

The El Hajan et al. [31] map defines the flow regimes and transitions based on mass flux and vapour quality. Knowing the flow regime means knowing what mechanisms are responsible for heat transfer and pressure drop [32].

The flow regimes identified as gravity-dominated are stratified and stratified-wavy flow, with condensate pools at the bottom of the tube due to the relatively low mass fluxes. Although these are two distinct flow regimes, from a heat transfer model point of view, they are treated using very similar forms of the same equations. In gravity-dominated flow, heat transfer is primarily due to the falling condensing film, while the liquid pool at the bottom decreases the heat transfer in that area.

The shear stress model is best utilised to represent the annular flow regime [33]. In this model, a thin liquid film wets the perimeter of the tube, which is in contact with a fast-moving vapour core. This flow is shear-dominated.

A large number of existing heat transfer correlations which are widely used, such as those of Dobson and Chato [34], Shah [35] and Thome et al. [36], were not specifically developed for application

Please cite this article in press as: E. van Rooyen et al., Probabilistic flow pattern-based heat transfer correlation for condensing intermittent flow of refrigerants in smooth horizontal tubes, Int. J. Heat Mass Transfer (2009), doi:10.1016/j.ijheatmasstransfer.2009.12.005

when the prevailing heat transfer mode is a combination of gravity-dominated and shear-dominated flow because these two categories were separated and treated individually. In fact, Thome et al. [36] state that even though they knew that the heat transfer performance in intermittent flow regime could not only be modelled using just a shear stress-based heat transfer correlation, they had no other available options. The intermittent flow regime defies classification by a single prevailing heat transfer mode [4] and might benefit from time-fractional probabilistic mapping to account for the inherent uncertainty in this region.

Two main methods of heat transfer in condensing two-phase flow in horizontal tubes have been identified, namely gravity-dominated and shear stress-dominated heat transfer [37,38]. The shortcomings of separating the two models for intermittent flow can be motivated by considering the use of a basic visual observation method to classify the flow. Depending on the instant of the observation, the appearance can either show gravity-dominated flow (with a liquid pool of condensate at the bottom) or shear stress-dominated flow (the liquid film is redistributed uniformly around the circumference of the tube). Thus, for intermittent flow, a single sample cannot determine the condition of the flow, which varies stochastically. Even a larger sample of multiple images is inconclusive, because the flow will appear different in each case.

A time-based probability model is defined here to overcome the problem of singular classification by combining the models for gravity- and shear stress-dominated flow. From a heat transfer perspective, this temporal variability in the flow might have a large effect that has not yet been quantified. Furthermore, a simple shear-controlled model (i.e. annular flow) or a gravity-controlled model will not suffice.

In this work, we present a heat transfer method for intermittent flow based on time-fractions. Due to the fact that the mathematical models for both gravity- and shear stress-dominated heat transfer modes have been defined separately, we attempt to decompose the intermittent flow regime so that the two separate heat transfer modes can be suitably applied to the prevailing flow conditions. The video image analysis used in the present study used light intensity fluctuations caused by the flow due to refraction, reflection and scattering of light to identify flow sub-regimes and not void fraction. The method is therefore simpler than neutron radiography and light extinction techniques.

The end result of a sub-mapped intermittent regime is the ability to apply a more local heat transfer correlation in the intermittent flow regime resulting in more accurate heat transfer predictions.

2. Experimental facility

The vapour-compression test facility consisted of two main subsystems: the vapour-compression loop, and the water cycles (Fig. 1). The vapour-compression cycle consisted of a hermetically sealed scroll compressor with a nominal cooling capacity of 10 kW. The condenser line splits up into two lines, namely the test line and the bypass line. Each line has its own electronic expansion valve (EEV). The test-line EEV was used to control the mass flux through the test line, and the bypass EEV was used to control the test pressure. The test line was comprised of four water-cooled condensers, a coiled tube-in-tube counterflow pre-condenser to control the inlet vapour quality, a straight horizontal tube-in-tube counterflow test heat exchanger, with water in the annulus and refrigerant on the inside, and two extra coiled tube-in-tube counterflow heat exchangers, namely the post-condenser and the subcooler. The post-condenser was utilised to control the post-condenser refrigerant state, which must be saturated liquid at the exit of the post. The

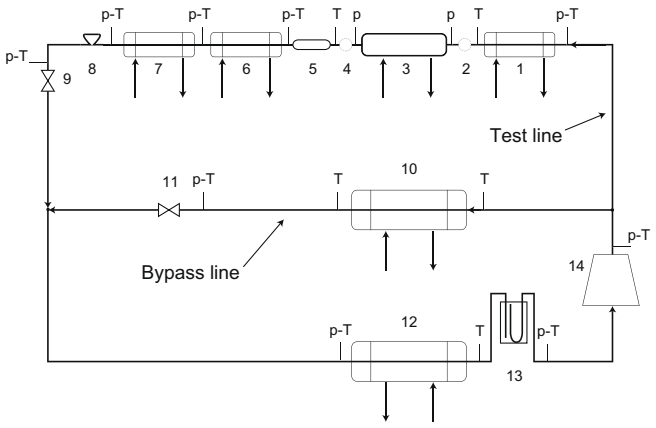

1. Pre-condenser (water-cooled)
2. Sight glass: high-speed videography
3. Test section (water-cooled)
4. Sight glass
5. Capacitive void fraction sensor
6. Post-condenser (water-cooled)
7. Sub-cooler (water-cooled)
8. Coriolis mass flow meter
9. Test line expansion valve
10. Bypass condenser (water-cooled)
11. Bypass line expansion valve
12. Evaporator (water-cooled)
13. Suction accumulator
14. Compressor

Fig. 1. Schematic diagram of the experimental layout for condensation experiments.

bypass line has one large water-cooled coiled tube-in-tube counterflow heat exchanger. After the expansion valves, the lines join up and go into the water-heated evaporator, which was followed by a suction-accumulator.

The test line was constructed of a 8.53 mm inner diameter copper tube. At the entrance of the test line, a straight calming section, 50 tube diameters long, was utilised to make sure the flow is fully developed [39]. Before the calming section is the pre-condenser, which was utilised to control the test section inlet vapour quality. A cylindrical sight glass was installed at the inlet of the test section, and was used to analyse the flow, using a high-speed camera. A calibrated, uniform Phlox backlight (98% uniform) was positioned against the sight glass and the camera, with an μ-tron FV2520 lens focused on 5 diameters of tube.

The inner-tube outer-wall temperatures of the 1.5 m long test section were measured at seven stations using four T-type thermocouples per station. A second sight glass was installed at the exit of the test section. These sight glasses were used not only for flow visualisation purposes, but also as insulators against thermal axial conduction of the copper tube. The sight glass inner diameter matches the copper tube inner diameter. The inlet and outlet temperatures of the inner tube were measured before the inlet and after the outlet sight glasses. All the thermocouples used in this experimental system were special limits of error specification and were calibrated against a high-precision Pt-100 resistance temperature device.

The absolute pressures of the condensing refrigerant were measured using Sensotech FP 2000 pressure transducers (3.4 MPa full scale), which were positioned at the inlet and outlet of the test section, between the sight glasses. A third, differential pressure transducer was connected between the inlet and the outlet of the test section to accurately measure the pressure drop. The refrigerant mass flow was measured using a Coriolis mass flow meter.

A capacitive void fraction sensor, developed by De Paepe et al. [40], was installed at the exit of the outlet sight glass, to measure the mean void fraction over the tube.

The oil concentration in the refrigerant was measured using the ASHRAE Standard [41], and a maximum of 2.3% was measured. This maximum of oil entrainment was only experienced at high

Please cite this article in press as: E. van Rooyen et al., Probabilistic flow pattern-based heat transfer correlation for condensing intermittent flow of refrigerants in smooth horizontal tubes, Int. J. Heat Mass Transfer (2009), doi:10.1016/j.ijheatmasstransfer.2009.12.005

mass fluxes. Shao and Granryd [42] showed that 2% oil entrainment in R-134a degraded the heat transfer coefficient by 10%, while Leibenberg et al. [43] showed that the Thome map can be used with oil in the refrigerant.

The water system was based on two insulated 5000 l tanks. The two tanks share a 70 kW heating/50 kW cooling dual-function heat pump and were thermostat-controlled between 13—17 °C and 23—27 °C, respectively, depending on the test requirements.

The water flow rates through the pre-, test and post-condensers were measured using separate Coriolis flow meters, while the ancillary heat exchangers' water mass flow rates were measured using gear-type flow meters. The inlet and outlet test-line heat exchangers' temperatures were measured using T-type thermocouples, also calibrated against a Pt-100 resistance temperature device.

Steady-state conditions were assumed when the energy balance error (Eq. (1)) was less than 1%, and the temperatures, pressures and mass flows of the system were constant for a period of at least 10 min. The fluctuation of the above mentioned measurements and other calculated properties were all statistically monitored for stability before testing. Further, experimental conditions were also maintained such that the vapour quality difference over the test section was less than 10% for semi-local heat transfer data [43]. This was done to minimise the uncertainty in the heat transfer measurements.

$$EB = \frac{Q_{ref} - Q_{water}}{Q_{ref}} \quad (1)$$

To test for repeatability (in the heat transfer measurements), three random points were selected from each test matrix and data were collected a second time, four weeks later. It was found that the results in terms of the heat transfer coefficient differed less than 5%.

The experimental uncertainties of the instruments are given in Table 1 and were calculated using the method described by Kline and McClintock [44].

3. Method

We have hypothesised that in a single flow regime, the two separate heat transfer modes (gravity and shear stress-dominated) will have an effect. The question is whether a more accurate heat transfer prediction method can be developed if we can classify the flow regimes so that for every mass flow rate and vapour quality we know the fractional probability of time that the flow will be in a dominant heat transfer mode.

In the method applied in this study a sample is a continuous measurement of image intensity over an area of sufficient size.

Table 1
Experimental uncertainties and test conditions.

Measured	Mean	Standard deviation	Uncertainty (%)
Refrigerant temperature			0.1 °C
Test line pressure			0.13
Inlet vapour quality			4.6
Heat transfer coefficient			13
Mass flux			0.6
Average heat flux			1
T_{sat}	39.7 °C	±1.9 °C	
EB	0.65%	±0.26%	
$\dot{m}_{ref}$	Test-dependent	Max: ± 2 kg/m^2 s	
Temperature per station	Test-dependent	0.11 °C	

The flow is characterised by means of a binomial classification in which intermittent flow can be classified as gravity or shear stress-dominated for each sample in the population and then on a time-fractional basis for the total sampling time. The probability function is a function of the probability that an intermittent flow at a specific condition of mass flux and vapour quality is gravity or shear stress-dominated ranging from 0 to 1. Thus we have a proposal for a statistically based probabilistic model of intermittent flow that can be applied to the flow pattern map to describe intermittent flow as gravity or shear stress-dominated. Later the probability function is renamed *tf* for time-fraction.

The link between two-phase flows and frequency content has long been investigated [45,4,16] among other. The method developed here proposes the use of time–frequency analysis and by adding the time component to the frequency analysis, the sub regimes present can be identified. This method can be applied to any form of measured properties that exhibits frequency characteristics in two-phase flow: pressure, void fraction and visual. The analysis of flow regimes was done by using of high-speed video recordings of the flow. The intensity of light that passed through the test section from the uniform backlight was used and time–frequency analysis was done on the intensity signal.

3.1. The analysis procedure

For the analysis of the high-speed recorded image sequences, a LabView program was used. The sequence of images was captured at 250 frames per second with an exposure of 1/5000 of a second and saved as an *.avi* file. The recordings were analysed by using an area of interest defined on the image. The height of the area was equal to a diameter and the width shorter than a quarter of the diameter. The mean light intensity was sampled as a function of 8 bit grayscale value in the area of interest during the sequence. A short-time Fourier transform was performed on each sample with a Gaussian window of width 32 after the signal was normalised and zero-padded.

For intermittent flow in general, the high-frequency activity represented annular flow or a liquid annulus with bubbles. From a light-intensity point of view, the larger number of liquid vapour interfaces and the unstable, wavy interfaces in these flows caused diffraction of the light and a rapid variation in light intensity. This was identified at frequencies above 25 Hz. The stratified and stratified-wavy flows resulted in less spectral activity and the largest variation of light intensity was due to the liquid vapour interface of the stratified layer. Gravity-dominated flow had frequency activity lower that 10 Hz. The time–frequency method applied to light intensity could thus, in a simple manner, improve objectivity in classifying flow patterns, especially in this case where a stochastic regime, namely intermittent flow, was being investigated.

The flows classified as annular flow were defined based on the premise that annular flow is a shear-dominated flow where gravity does not play a large role and this corresponded to high-frequency activity due to the large amount of light fluctuations. The stratified regimes are flows where gravity has a significant influence on the flow pattern and were characterised by low-frequency activity due to the low amount of light scattering activity.

3.2. Data reduction

The properties of the refrigerant at the inlet of the pre-condenser and outlet of the post-condenser were determined by temperature and pressure measurements. From these measurements, the thermophysical properties of the condensing refrigerant were

Please cite this article in press as: E. van Rooyen et al., Probabilistic flow pattern-based heat transfer correlation for condensing intermittent flow of refrigerants in smooth horizontal tubes, Int. J. Heat Mass Transfer (2009), doi:10.1016/j.ijheatmasstransfer.2009.12.005

determined by utilising data from a refrigerant property database [46,47].

However, due to the fact that the inlet and outlet of the test section are in the saturated regime, it is not possible to use only the measured temperature and pressure signals to obtain the thermophysical properties. For this reason, the system energy balance is calculated using the heat transferred out of the refrigerant from the inlet of the pre-condenser (superheated), to the outlet of the post-condenser (subcooled), and the sum of the heat transferred into the water-side of the three heat exchangers. Due to the fact that it is not possible to measure the heat transferred out of the refrigerant line over the test section directly, an energy balance error of less than 1% was obtained before the water-side heat transfer is utilised to calculate the outlet refrigerant properties. The same principle is also valid for the pre-condenser. The average inlet and outlet vapour qualities are obtained using

$$x_j = \frac{h_j - h_{L,j}}{h_{V,j} - h_{L,j}} \text{ with enthalpies } h_L \text{ and } h_V \text{ measured at temperature } T_j \tag{2}$$

In the above equation, j is utilised to denote either the inlet or outlet of the test section. The values of the enthalpy were calculated using

$$h_j = h_k - \left| \frac{\dot{Q}_{kj}}{\dot{m}_{ref}} \right| \tag{3}$$

In the above equation, k denotes the position prior to position j. Thus if calculating the test inlet vapour quality, k denotes the precondenser refrigerant inlet, while if the test outlet vapour quality is calculated, k denotes the inlet of the test section.

The heat transfer coefficient is calculated using the mean wall temperature of the test section, the heat transferred into the water-side of the test section, and the mean refrigerant temperature between the inlet and the outlet. To calculate the mean wall temperature of the test section the distance between stations is also taken into account by using the trapezium numerical integration method, ensuring that any non-linearity in temperature distribution over the length of the tube wall can be reflected in a more representative average. This is

$$T^m_{w,o} = \frac{1}{L} \sum_{j=1}^{6} \left[\frac{1}{2} (T^j_{w,o} + T^{j+1}_{w,o})(x_{j+1} - x_j) \right] \tag{4}$$

Utilising this averaging method when the temperature drop is linear results in the same average as a normal mean of all the temperature readings. The inner wall temperature, such that the proper temperature difference may be calculated, is

$$T^j_{w,i} = T^j_{w,o} + \left| \dot{Q}_{H_2O} \cdot R_w \right| \tag{5}$$

Where the wall thermal resistance, R_w is

$$R_w = \frac{\ln \frac{d_{i,o}}{d_{i,i}}}{2\pi k_{Cu} L} \tag{6}$$

The thermal conductivity of the tube is calculated as a function of temperature [48]. The heat transfer on the water-side is utilised along with the inside heat transfer area. Then, the semi-local experimental convective heat transfer coefficient is

$$h_{c,exp} = \left| \frac{\dot{Q}_{H_2O}}{A_L(\overline{T}_{w,i} - \overline{T}_{b,m})} \right| \tag{7}$$

For the probabilistic time-fraction map the analysed data is presented as a time-fractional function (tf). The value of tf varies from 0 (gravity-dominated) to 1 (shear stress-dominated) and was presented as a function of mass flux and vapour quality. It is presented as function of vapour quality rather than void fraction to accommodate the heat transfer model mentioned in Section 4, and the Thome prediction method [36].

4. Time fraction-corrected heat transfer correlation

The ability to determine the probability that, at a certain mass flow rate and vapour quality, a certain heat transfer mode will prevail can directly aid in increasing the accuracy of existing heat transfer correlations. This can be done not by changing the leading coefficients and exponents for ones that better fit the experimental data, but by better describing the physics of the flow. The time-fraction map is based on the assumption that for every single point in the time-fraction map the heat transfer dominance is shifted from gravity-based to shear stress-based in a linear fashion. This is to say that if tf fraction of the time is spent in shear stress-dominated heat transfer mode, then $(1 - tf)$ will be spent in the gravity-dominated heat transfer mode.

We can begin by postulating that the time fraction-corrected heat transfer coefficient in the intermittent flow regime would be a binomial combination of the gravity- and shear stress-based heat transfer coefficients. This is not to say that intermittent flow is a linear combination of flows because the tf function remains non-linear.

$$h_{c,tf} = tf \cdot h_{c,shear} + (1 - tf) \cdot h_{c,grav} \tag{8}$$

where $h_{c,shear}$ and $h_{c,grav}$ are calculated from the Thome et al. [36] correlation. Namely,

$$h_{c,shear} = 0.003 Re_L^{0.74} Pr_L^{0.5} \frac{k_L}{\delta} f_i \tag{9}$$

where the interfacial correction factor f_i and the film thickness δ are, respectively

$$f_i = 1 + \left(\frac{u_V}{u_L} \right)^{\frac{1}{2}} \left(\frac{(\rho_L - \rho_V) g \delta^2}{\sigma} \right)^{\frac{1}{4}} \tag{10}$$

$$\delta = \frac{d(1 - \varepsilon)}{4} \tag{11}$$

and ε is

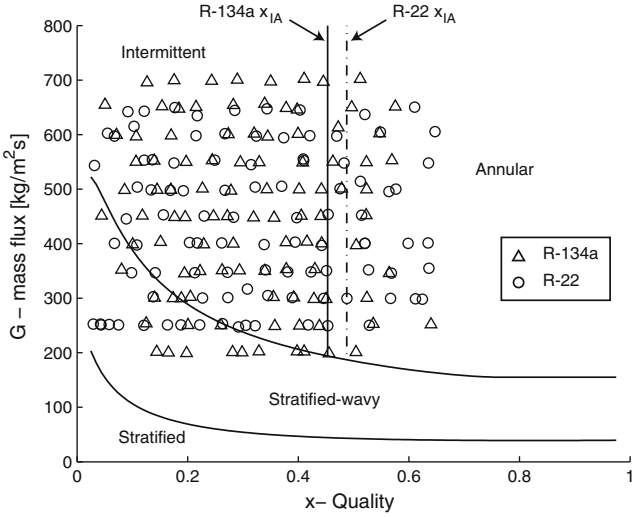

Fig. 2. Experimental test points overlaid on the Thome-El Hajal flow map [31] for refrigerant condensing in an 8.38 mm ID smooth tube, at a nominal saturation temperature of 40 °C.

Please cite this article in press as: E. van Rooyen et al., Probabilistic flow pattern-based heat transfer correlation for condensing intermittent flow of refrigerants in smooth horizontal tubes, Int. J. Heat Mass Transfer (2009), doi:10.1016/j.ijheatmasstransfer.2009.12.005

$$\varepsilon = \frac{\varepsilon_h - \varepsilon_{ra}}{\ln \frac{\varepsilon_h}{\varepsilon_{ra}}} \tag{12}$$

The homogeneous void fraction, ε_h, is

$$\varepsilon_h = \left[1 + \left(\frac{1-x}{x}\left(\frac{\rho_V}{\rho_L}\right)\right)\right]^{-1} \tag{13}$$

and the Rouhani–Axelsson void fraction, ε_{ra},

$$\varepsilon_{ra} = \frac{x}{\rho_V}\left([1+0.12(1-x)]\left[\frac{x}{\rho_V}+\frac{1-x}{\rho_L}\right]+\frac{1.18(1-x)[g\sigma(\rho_L-\rho_V)]^{0.25}}{G\rho_L^{0.5}}\right)^{-1} \tag{14}$$

In the case of the gravity-based heat transfer correlation, the heat transfer coefficient is

$$h_{c,grav} = \frac{h_f r\theta + (2\pi-\theta) r h_{c,shear}}{2\pi r} \tag{15}$$

$h_{c,shear}$ is the same heat transfer correlation shown in Eq. (9). The turbulent film heat transfer coefficient is found using

$$h_f = 0.728\left[\frac{\rho_L(\rho_L-\rho_V)g h_{LV} k_L^3}{\mu_L d_{i,i}(T_{sat}-T_w)}\right]^{\frac{1}{4}} \tag{16}$$

The falling film angles θ and θ_{strat}, according to the original Thome et al. [36] formulation are

$$\theta = \theta_{strat}\left(\frac{G_{wavy}-G}{G_{wavy}-G_{strat}}\right)^{0.5} \tag{17}$$

$$\theta_{strat} = 2\pi - 2\left\{\begin{array}{l}\pi(1-\varepsilon)+\left(\frac{3\pi}{2}\right)^{\frac{1}{3}}[1-2(1-\varepsilon)+(1-\varepsilon)^{\frac{1}{3}}-\varepsilon^{\frac{1}{3}}] \\ -\frac{1}{200}(1-\varepsilon)\varepsilon[1-2(1-\varepsilon)][1+4((1-\varepsilon)^2+\varepsilon^2)]\end{array}\right\} \tag{18}$$

In Eq. (17), the term in brackets is a proration between the transitions of stratified and stratified-wavy flow. If the mass flux is increased over the limit of G_{wavy} (as would occur if we attempted a proration into the intermittent flow regime), θ would become non-sensical (due to trying to take the square root of a negative number). Thus, we have set $\theta = \theta_{strat}$ to maintain the gravity-dominated heat transfer coefficient at mass fluxes higher than G_{wavy}. This is to say that the falling film angle θ is made equal to the stratification angle θ_{strat} for all applications in the time-fractional formulation. Complete information on the factors influencing Eq. (17) is given in [36]. Furthermore, since the values of G_{wavy} and G_{strat} are not utilized for this method, they are not presented in this text. These are also presented in [36].

5. Results

A total of 203 data points were captured in a smooth horizontal tube section for R-22 and R-134a ranging in mass flux from 200 up to 700 kg/m^2 s, and with a vapour quality varying between 0.05 and 0.65, as shown in Fig. 2. Most data points are in intermittent flow but it was required that some data points fall into what Thome et al. [36] defines as the stratified-wavy regime and the annular flow regime. The mean test data for the data points and the experimental uncertainties are summarised in Table 1.

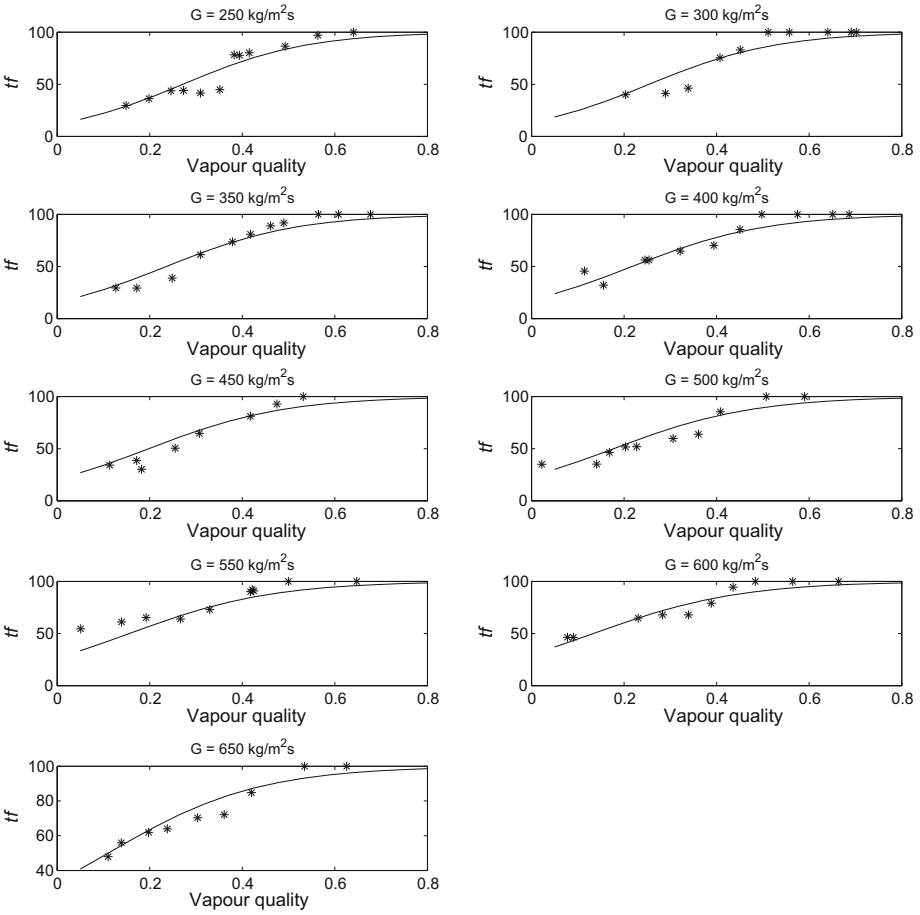

Fig. 3. The time fraction (tf) analysis results for refrigerant mass fluxes from 250 to 650 kg/m^2 s tested with R-22 during condensation at 40 °C. The tf is the solid line and * are measurements.

Please cite this article in press as: E. van Rooyen et al., Probabilistic flow pattern-based heat transfer correlation for condensing intermittent flow of refrigerants in smooth horizontal tubes, Int. J. Heat Mass Transfer (2009), doi:10.1016/j.ijheatmasstransfer.2009.12.005

Table 2
Binomial general linear model function coefficients.

Refrigerant	a_1	a_2	b_1	b_2	R^2
R-22	0.0033	−2.8251	−0.003	8.1182	0.86
R-134a	0.004	−2.9502	0.0071	3.6698	0.85

The results are given here by presenting the time-fractional maps first and then the heat transfer data.

5.1. Time-fractional results

The function that suited the nature of the time-fractional data best was a generalised linear model with binomial distribution. This function is suited for populations that are sampled as a fraction of a total. In this case, the total was 100% shear dominated flow and this tended to $tf = 1$ for fully annular flow where tf is the time-fractional value. The time-fractional data were used in combination with the flow conditions and a non-linear least squares optimisation algorithm to solve for the coefficients of a best fit. The function used is defined in Eq. (21) and the results are given in Fig. 3. The functions describe the data with a R^2 of 85% over the test range.

$$a = a_1 * G + a_2 \tag{19}$$

$$b = b_1 * G + b_2 \tag{20}$$

$$y^* = a + bx$$

$$\text{so that } (tf) = g'(y^*) \tag{21}$$

$$\text{where } g(\mu) = \ln\frac{\mu}{1-\mu}$$

The function coefficients for the time-fraction data fit with Eq. (21) are presented in Table 2. The results described here are based on experimental data from two refrigerants, a single diameter and saturation temperature. It was never applied outside of these conditions.

The raw data from the analysis are given together with the tf function for R-22 (Fig. 3) and R-134a (Fig. 4). A section of the function at each tested mass flux range is given for R-22 (Fig. 5) and R-134a (Fig. 6).

In general, the low vapour qualities and mass fluxes resulted in the lower time-fractions and thus more gravity-dominated flows. The higher mass fluxes resulted in higher time-fractions indicating more shear stress-dominated flows. There was no significant drop in tf at higher mass fluxes, as the vapour quality decreased, indicating the persistence of shear effects.

The difference between the two refrigerants can also be noted by the different slopes of the functions and the different magni-

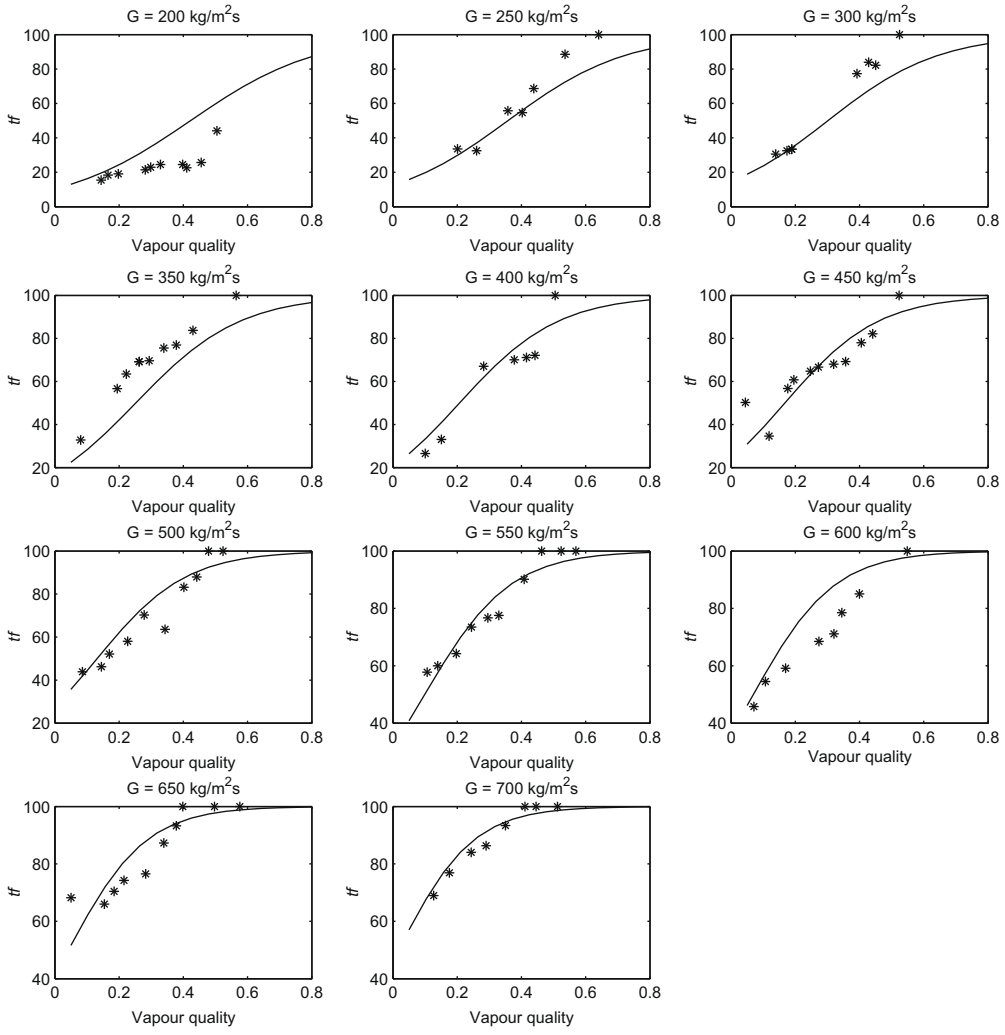

Fig. 4. The time fraction (tf) analysis results for refrigerant mass fluxes from 200 to 700 kg/m^2 s tested with R-134a during condensation at 40 °C. The tf is the solid line and * are measurements.

Please cite this article in press as: E. van Rooyen et al., Probabilistic flow pattern-based heat transfer correlation for condensing intermittent flow of refrigerants in smooth horizontal tubes, Int. J. Heat Mass Transfer (2009), doi:10.1016/j.ijheatmasstransfer.2009.12.005

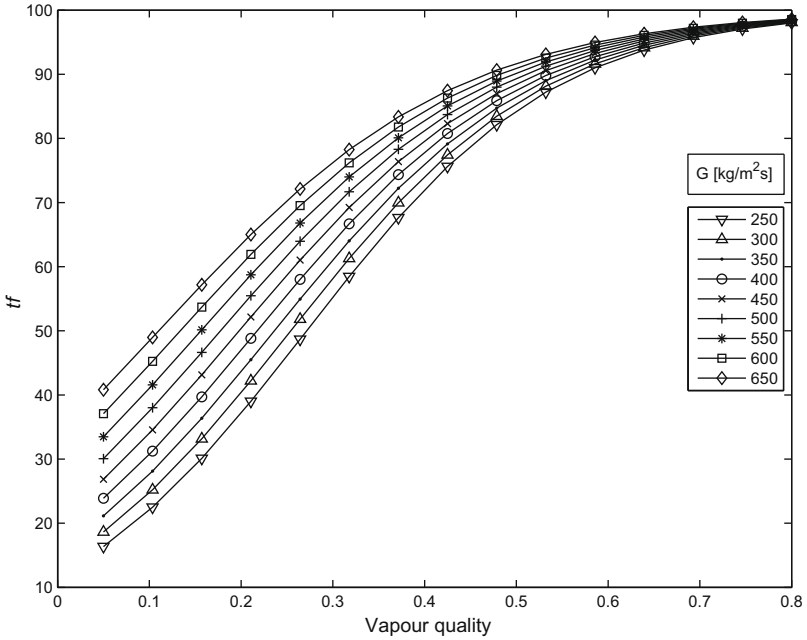

Fig. 5. Time-fractional results combined for condensing refrigerant tests with R-22 at 40 °C.

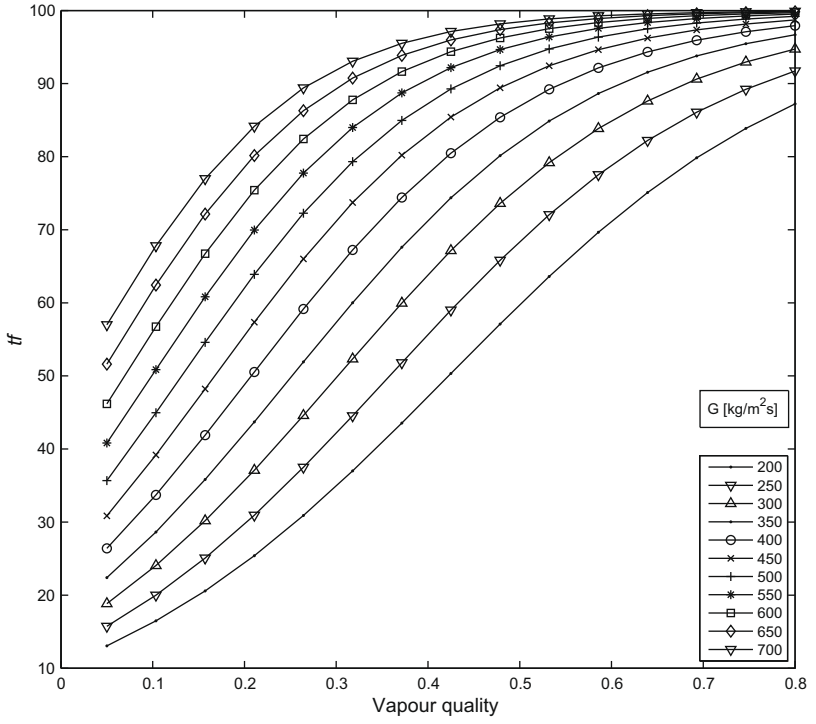

Fig. 6. Time-fractional results combined for condensing refrigerant tests with R-134a at 40 °C.

tudes of *tf*. The R-134a has a slightly higher tendency to higher *tf* values (shear stress-dominated) and at lower vapour quality compared with R-22 (Fig. 7). The Thome-El Hajal flow pattern map also indicates a lower vapour quality threshold (more shear stress-dominated flow) for annular flow with the x_{ia} transition at 45% for R-134a and at 49% for R-22 (Fig. 2). According to the refrigerant properties given in Table 3, the only significant difference is in viscosity with minor differences in reduced pressure, density and density ratio.

Based on the time-fractions and visual observations it was noted that there is a change in the dominant flow patterns from a shear-dominated annular film-type of flow to a gravity-dominated stratified-type of flow at lower vapour qualities. This occurs at vapour qualities less than 0.25 and is an intermittent occurrence that is noticeable in the region from 0.10 to 0.25 vapour quality.

This occurrence at lower vapour qualities is likely the reason for many flow pattern maps, when compared with the Thome flow map, to have a transition line defined at the location of 0.1–0.25

Please cite this article in press as: E. van Rooyen et al., Probabilistic flow pattern-based heat transfer correlation for condensing intermittent flow of refrigerants in smooth horizontal tubes, Int. J. Heat Mass Transfer (2009), doi:10.1016/j.ijheatmasstransfer.2009.12.005

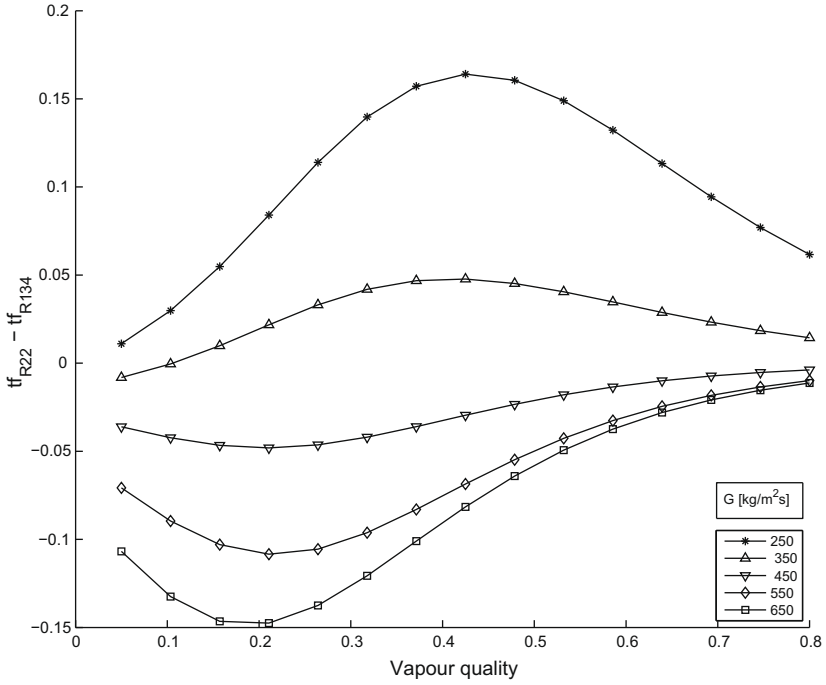

Fig. 7. Comparison of time-fractional functions for R-22 and R-134a condensing at 40 °C indicating the difference of the two *tf* functions as $tf_{R-22} - tf_{R-134a}$.

vapour quality [31]. Cavallini et al. [30] defined a heat transfer prediction method based on the temperature dependence of the prevailing flow regime. The flow pattern map of Cavallini et al. [29] defines a transition through the intermittent flow regime at the mentioned location. According to their transition, annular flow is more persistent at high mass fluxes during condensation. The Tandon et al. [49], Soliman [50] and Dobson and Chato [34] flow pattern maps have similar transitions and are discussed by El Hajan et al. [31]. The transition line that these methods predict is not consistent because there is large room for interpretation in the ambiguous intermittent flow regime.

These flow pattern maps all attempt to predict a transition that is based on stochastic behaviour, which is difficult to classify. The subjectivity in discriminating between these flow patterns leads to the variation of the predicted transition. The time-fractional method does not attempt to define this boundary with a single function but rather to represent the actual flow behaviour and to model the flow based on a continuous time-fractional function of statistical origin.

5.2. Experimental heat transfer coefficient results

Fig. 8 presents the raw experimental data found in this study against those found by Cavallini et al. [51] for R-134a for a tube of similar size, as well as similar operating conditions. The solid circles represent the data found by Cavallini et al. [51], while the rest of the symbols are the experimental data points found in this study, separated by mass flux. When compared against the data found by Cavallini et al. [51], the experimental data found in this campaign shows the same increasing trend with increasing vapour quality. Furthermore, it can be seen that the experimental data from both campaigns are well clustered. The only data that does not correspond to the general trends shown are the three points of Cavallini et al. [51] at a vapour quality of 0.3($h_c = \pm 4500$ W/m^2 K). The reason for this is not clear.

Table 3
Refrigerant properties for R-22 and R-134a at 40 °C [47].

	R-22	R-134a	Unit
Temperature	40	40	°C
Pressure	1530	1012	kPa
Critical pressure	5000	3600	kPa
Reduced pressure	0.3	0.27	–
Liquid viscosity	138.9	161.8	μPa s
Vapour viscosity	13.34	12.3	μPa s
Surface tension	0.0061	0.0061	N/m
Liquid density	1130	1150	kg/m^3
Vapour density	66	50	kg/m^3
Density ratio	0.0575	0.0434	–
x_{ia}	0.49	0.46	–

Fig. 9 presents the experimental heat transfer coefficient against the Thome et al. [36] correlation. Measurements, with oil, by Leibenberg et al. [43] were successfully compared against the Thome-El Hajal map. The values for the Thome heat transfer coefficient were calculated utilising the required heat transfer coefficient form, depending on the flow regime in which the data point was situated.

The mean percentage deviation of the experimental heat transfer coefficient with respect to the Thome correlation's heat transfer coefficient is −1%; the absolute mean percentage deviation is 15%, while the standard deviation of this mean was found to be ±10.5%. The mean deviation shows that the experimental data from the system is overpredicted as much as it is underpredicted by the correlation of Thome et al. [36]. This can be seen in Fig. 9.

Carrying on with the analysis, the time fraction-corrected heat transfer coefficient was calculated. Fig. 10 shows the experimental heat transfer coefficient plotted against the time fraction-corrected heat transfer coefficient correlation.

The experimental results' mean percentage deviation when compared with the time fraction-corrected heat transfer correlation is, on average, −5.2%. While the mean percentage deviation has increased, the absolute mean deviation percentage decreased to 10%, and the standard deviation of this mean is ±7.5%. When evaluating Fig. 10, it follows that the points that were at the lower range of both mass flux (200–300 kg/m^2 s) and vapour quality, which were both underpredicted by the (classical) Thome correlation, are now within ±25% of the measured value.

Please cite this article in press as: E. van Rooyen et al., Probabilistic flow pattern-based heat transfer correlation for condensing intermittent flow of refrigerants in smooth horizontal tubes, Int. J. Heat Mass Transfer (2009), doi:10.1016/j.ijheatmasstransfer.2009.12.005

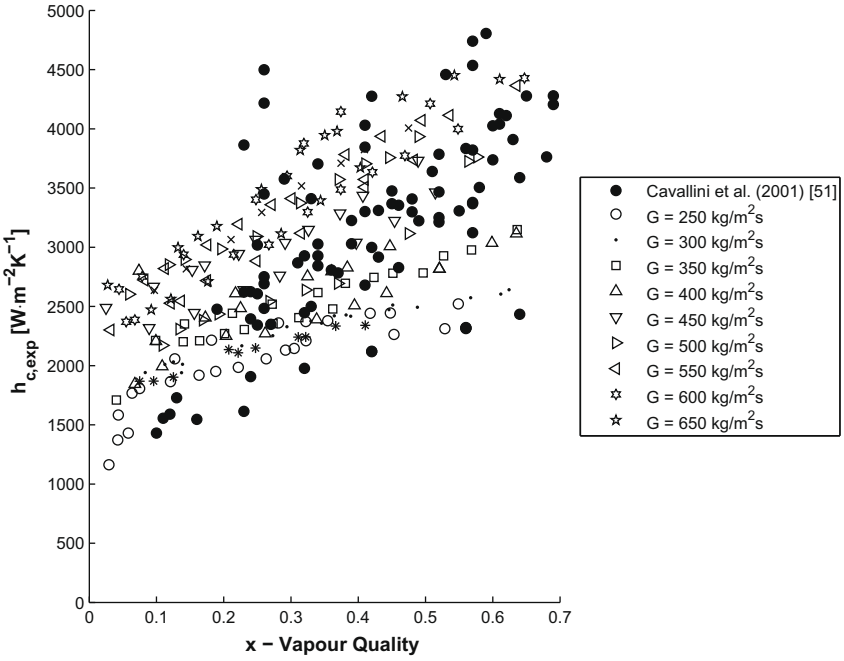

Fig. 8. Experimental heat transfer results comparison with experimental data gathered by Cavallini et al. [51].

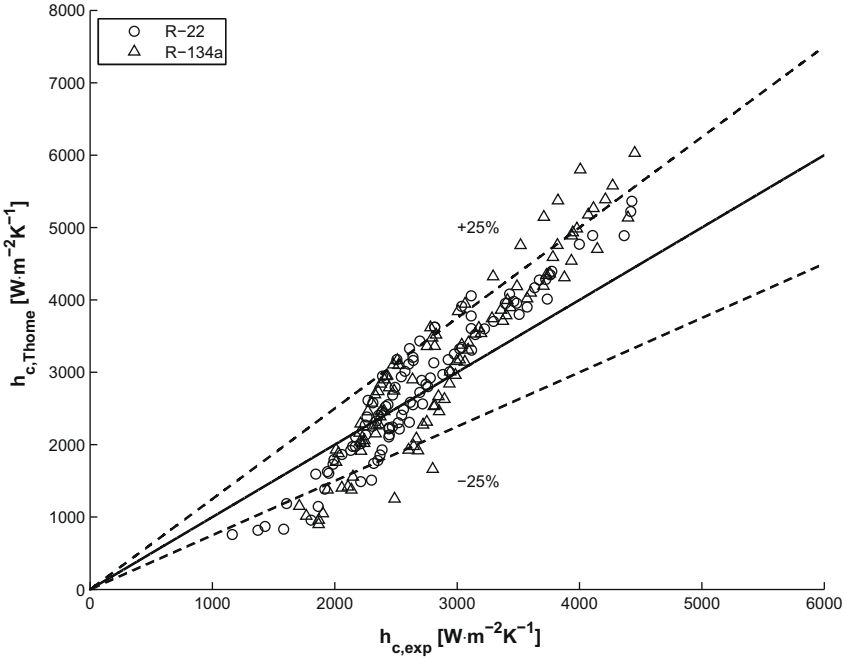

Fig. 9. Experimental heat transfer results comparison with the Thome et al. [36] correlation.

Fig. 11 shows the experimental heat transfer coefficients compared with both the time fraction-corrected heat transfer and the (classical) Thome correlation [36] for constant mass fluxes of 200 and 250 kg/m^2 s. The mean absolute percentage deviation between the time fraction-corrected heat transfer coefficients and the experimental results drop to 7.5%. In contrast, for the same mass flux, the experimental results' mean deviation from the Thome heat transfer coefficient predictions [36] is 25%.

On a point-by-point direct comparison between the prediction of the time fraction-corrected model and the Thome prediction [36], it follows that the points at lower vapour qualities benefited the most from the application of the time fraction data. Furthermore, in the method proposed by Thome et al. [36], the heat transfer correlation for annular flow is extended into the intermittent flow regime; however, the time fraction results clearly show that as the vapour quality decreases, the probability of finding shear-dominated flow also decreases.

The influence of the time-fraction decreases as the vapour quality increases and the heat transfer coefficient increases since the flow regime tends towards the annular flow regime. At

Please cite this article in press as: E. van Rooyen et al., Probabilistic flow pattern-based heat transfer correlation for condensing intermittent flow of refrigerants in smooth horizontal tubes, Int. J. Heat Mass Transfer (2009), doi:10.1016/j.ijheatmasstransfer.2009.12.005

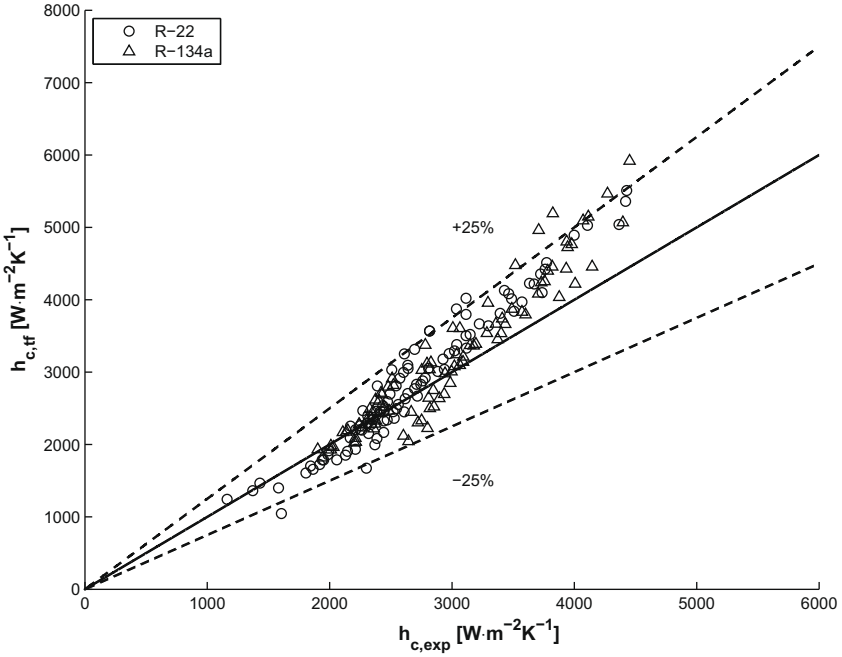

Fig. 10. Comparison of experimental heat transfer coefficients with the suggested time fraction-corrected heat transfer prediction.

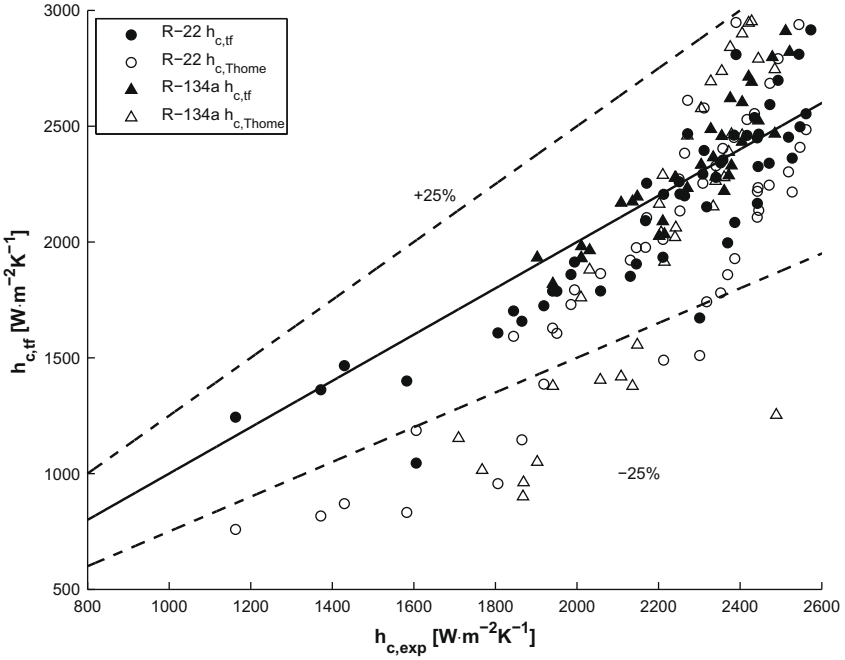

Fig. 11. Comparison of the experimental heat transfer coefficients with predicted data at G = 200 and 250 kg/m^2 s.

these conditions the annular flow heat transfer prediction and the prediction of the time-fraction method are similar. Thus, at higher vapour qualities (and mass fluxes), the shear stress-based heat transfer coefficient becomes dominant, as shown in Fig. 12.

The measurements at 300, 350 and 400 kg/m^2 s are presented in Fig. 13. The heat transfer coefficients at the lower qualities show the best improvement. At these mass fluxes, the shear stress and gravity heat transfer coefficient values, as depicted in Fig. 12, are very close to each other, which is why the time fraction-corrected points do not vary very much from their Thome counterparts.

Starting at mass fluxes higher than 450 kg/m^2 s, the time fraction goes to high levels faster than at lower mass fluxes, which means that the number of data points that are heavily affected by the time fraction correction decreases. For example, at $G = 450$ kg/m^2 s, half of the data points are very near their Thome counterparts, all of these at the higher vapour qualities, while the meaningful prediction corrections are still effected at lower vapour

Please cite this article in press as: E. van Rooyen et al., Probabilistic flow pattern-based heat transfer correlation for condensing intermittent flow of refrigerants in smooth horizontal tubes, Int. J. Heat Mass Transfer (2009), doi:10.1016/j.ijheatmasstransfer.2009.12.005

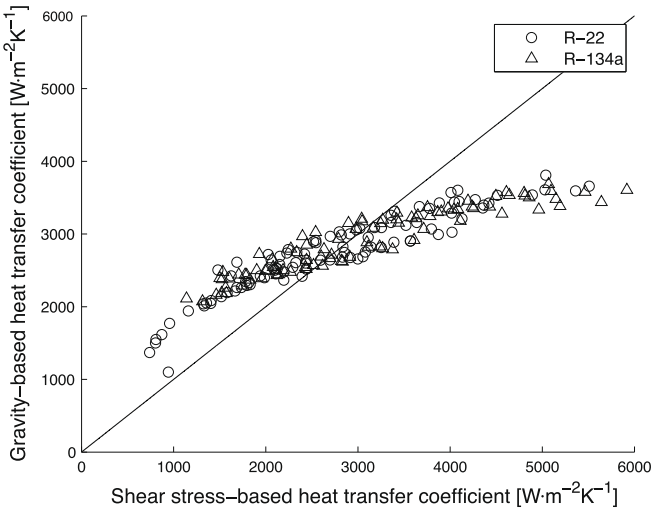

Fig. 12. Comparison of shear stress-based and gravity-based coefficient dominance.

qualities. Furthermore, at vapour qualities still in the intermittent flow but not close to the intermittent-annular transition curve, the influence of the gravity term is attenuated, generating results similar to those found with the Thome correlation at high mass fluxes.

At the mass fluxes of 600, 650 and 700 kg/m^2 s (Fig. 14) the shear stress-based prediction is high compared to the gravity-based coefficient. Coupled with the reduced influence of the time-fraction this ends up with a heat transfer coefficient prediction similar to the Thome correlation.

The time fraction method was also compared to the method described by Jassim et al. [8], in which a flow regime-based condensation model was developed for several refrigerants in a single, horizontal, smooth tube utilizing a probabilistic two-phase flow map. The authors also defined a time fraction (in a different manner than in this paper) to provide weighting of heat transfer models developed for the different flow regimes. In Fig. 15, predictions from the model developed by Jassim et al. [8] and the method developed in this study are calculated using, as inputs, the experimental conditions found in the campaign detailed in this study. On cursory inspection, both models predict the data reasonably well. However, it can be seen that there is a larger discrepancy between the two models' predictions of the R-22 heat transfer performance. To further study, the two models are plotted against the experimental data, again separated by refrigerant used, in Fig. 16. The absolute mean percentage deviations of the correlation developed in this study are, for R-22 and R-134a, respectively, 11% and 10% (these values have already been presented and discussed previously). For the method developed by Jassim et al. [8], the R-134a absolute mean percentage deviation to the experimental data presented here is 12%; however, for the R-22 data, this value is 33%, evidenced in the large divergence at higher heat transfer coefficients. The reason for this is unclear, as this method was developed using R-22 as one of the test refrigerants. Nonetheless, it is interesting to note that at the lowest mass fluxes, the method proposed by Jassim et al. [8] and that proposed by this study show the same flat trend (in Fig. 16, the values between 1000 and 2000 W/m^2 K on the *x*-abscissa). This might imply that the underlying physics of the two prediction methods are similar.

6. Conclusion

In the study condensation testing on R-22 and R-134a was done for two-phase intermittent flow. The analysis method described above and used in this study is based on measuring the light intensity passing through a sight glass followed by a time–frequency analysis on the signal. The time-fractional analysis technique was intended to provide a tool for objective analysis of two-phase flow and identifying the sub-regimes of gravity-dominated and shear stress-dominated flow.

The most debated transition in condensing flow is in the intermittent flow regime where no single transition coincides with another. The method used here does not propose the use of a fixed transition line between two flow regimes. It is proposed to use a probabilistic approach that statistically describes the mix of

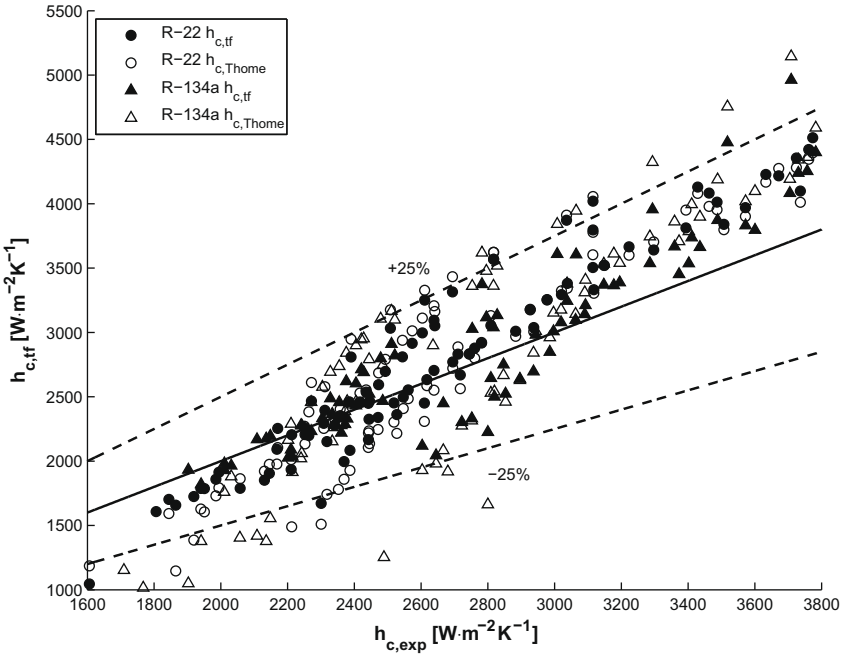

Fig. 13. Comparison of the experimental heat transfer coefficients with predicted data at G = 300, 350 and 400 kg/m2 s.

Please cite this article in press as: E. van Rooyen et al., Probabilistic flow pattern-based heat transfer correlation for condensing intermittent flow of refrigerants in smooth horizontal tubes, Int. J. Heat Mass Transfer (2009), doi:10.1016/j.ijheatmasstransfer.2009.12.005

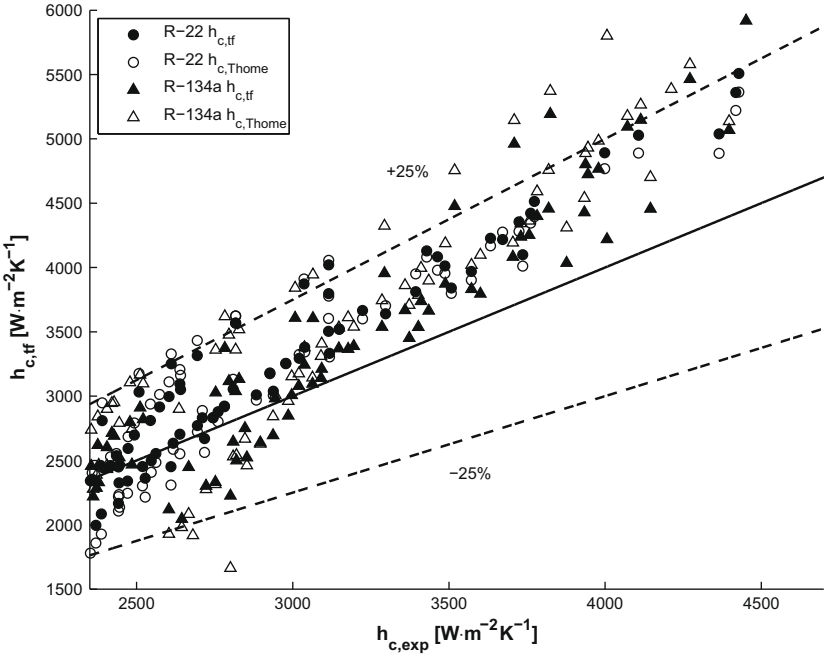

Fig. 14. Comparison of the experimental heat transfer coefficients with predicted data at $G = 600$, 650 and 700 kg/m^2 s.

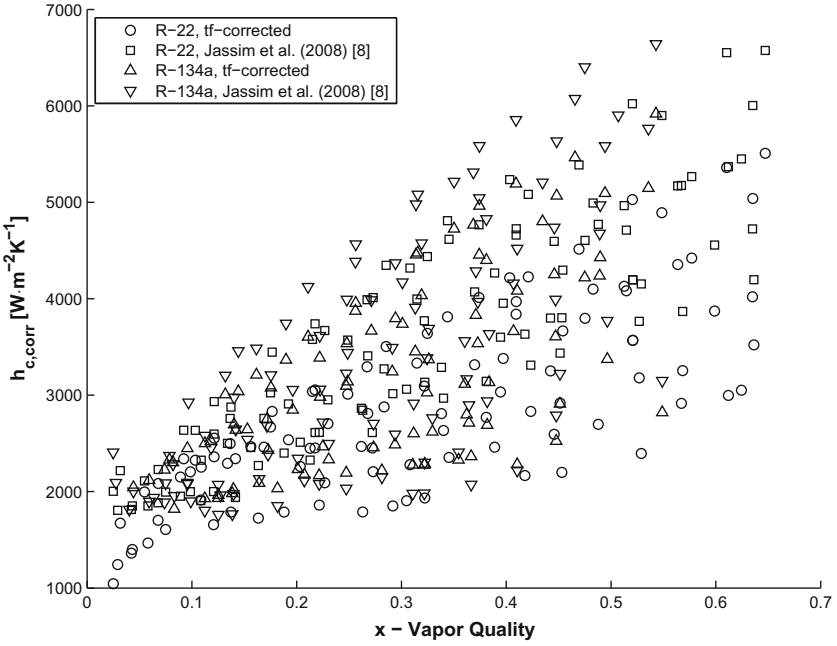

Fig. 15. Predictions from the Jassim et al. [8] method and the Thome et al. [36] based time fraction method developed in this study, calculated using the same inputs (from experimental conditions).

dominant flow patterns present in intermittent flow. This approach does not result in any discontinuities and blends in with the existing model of Thome without problems.

The flow pattern detection method developed and applied to identify the difference in flow patterns worked well and could successfully detect minor variations in two-phase flow allowing the method to be applied in sub-mapping the intermittent flow regime for mass fluxes less than 700 kg/m^2 s.

The time-fraction was combined with the two flow regime-based correlations to create a time fraction-corrected flow pattern-based heat transfer correlation for the intermittent flow regime, in an successful effort to better predict the heat transfer behaviour in this regime. The method is based on actual physical behaviour of the flow. It was shown that the time fraction correction has more effect when the vapour quality is low, and especially so when the mass flux is also relatively low ($G = 200$ and

Please cite this article in press as: E. van Rooyen et al., Probabilistic flow pattern-based heat transfer correlation for condensing intermittent flow of refrigerants in smooth horizontal tubes, Int. J. Heat Mass Transfer (2009), doi:10.1016/j.ijheatmasstransfer.2009.12.005

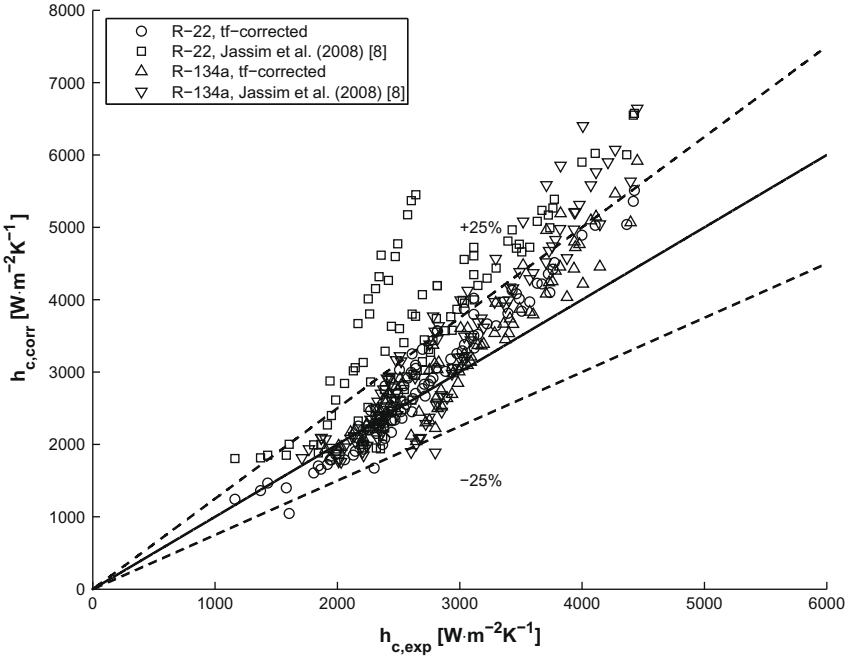

Fig. 16. Comparison of the Thome et al. [36] based time fraction method developed in this study with the Jassim et al. [8] correlation.

300 kg/m^2 s) due to the correction of the shear stress-based prediction.

Acknowledgements

This work was supported by the National Research Foundation (NRF) and Eskom (TESP).

References

[1] J. Keska, M. Smith, B. Williams, Comparison study of a cluster of four dynamic flow pattern discrimination techniques for multi-phase flow, Flow Meas. Instrum. 10 (1999) 65–77.
[2] G. Kirouac, T. Trabold, P. Vassallo, W. Moore, R. Kumar, Instrumentation development in two-phase flow, Exp. Thermal Fluid Sci. 20 (1999) 79–93.
[3] D. Lowe, K. Rezkallah, Flow regime identification in microgravity two-phase flows using void fraction signals, Int. J. Multiphase Flow 25 (1999) 433–457.
[4] L. Liebenberg, J. Meyer, The characterization of flow regimes with power spectral density distributions of pressure fluctuations during condensation in smooth and micro-fin tubes, Exp. Thermal Fluid Sci. 31 (2006) 127–140.
[5] J.R. Thome, Update on advances in flow pattern based two-phase heat transfer models, Exp. Thermal Fluid Sci. 29 (2005) 341–349.
[6] V. Niño, P. Hrnjak, T. Newell, Characterization of two-phase flow in microchannels, Air Conditioning Refrig. Center 107 (2002) 1–97.
[7] E. Jassim, T. Newell, J. Chato, Probabilistic determination of two-phase flow regimes in horizontal tubes utilizing an automated image recognition technique, Exp. Fluids 42 (2007) 563–573.
[8] E. Jassim, T. Newell, J. Chato, Prediction of two-phase condensation in horizontal tubes using probabilistic flow regime maps, Int. J. Heat Mass Transfer 51 (3–4) (2008) 485–496.
[9] R. Revellin, V. Dupont, T. Ursenbacher, J.R. Thome, I. Zun, Characterization of diabatic two-phase flows in microchannels: flow parameter results for R-134a in a 0.5 mm channel, Int. J. Multiphase Flow 32 (2006) 755–774.
[10] H. Canière, C. T'Joen, A. Willockx, M.D. Paepe, Capacitance signal analysis of horizontal two-phase flow in a small diameter tube, Exp. Thermal Fluid Sci. 32 (3) (2008) 892–904.
[11] H. Canière, B. Bauwens, C. T'Joen, M.D. Paepe, Probabilistic mapping of adiabatic horizontal two-phase flow by capacitance signal feature clustering, Int. J. Multiphase Flow 35 (7) (2009) 650–660.
[12] K. Mishima, T. Hibiki, H. Nishihra, Visuaization and measurement of two-phase flow by using neutron radiography, Nucl. Eng. Des. 175 (1997) 25–35.
[13] K. Mishima, T. Hibiki, Some characteristics of air–water teo-phase flow in small diameter vertical tubes, Int. J. Multiphase Flow 22 (1996) 703–712.
[14] B. Shamoun, M. Beshbeeshy, R. Bonazza, Light extinction technique for void fraction measurements in bubbly flow, Exp. Fluids 26 (1999) 16–26.
[15] J. Berthold, S. Reed, C. Nash, Fibre optic sensor system for void fraction measurement in aqueous two-phase fluids, Flow Meas Instrum 5 (1994) 3–13.
[16] E. Hervieu, P. Seleghim, An objective indicator for two-phase flow pattern transition, Nucl. Eng. Des. 184 (1998) 421–435.
[17] F. Klein, P. Seleghim, E. Hervieu, Time–frequency analysis of intermittent two-phase flows in horizontal piping, J. Braz. Soc. Mech. Sci. XXVI (2004) 174–179.
[18] MIT Opencourseware, OpenCourseWare: Short-time Fourier Analysis, 2006.
[19] Mathworks, Matlab R15, Reading, 2005.
[20] L. Liebenberg, A. Bergles, J. Meyer, A review of refrigerant condensation in horizontal micro-fin tubes, Proc. ASME Adv. Energy Syst. Div. (2001) 155–168.
[21] L. Cheng, G. Ribatski, J.R. Thome, New prediction methods for CO_2 evaporation inside tubes. Part II – An updated general flow boiling heat transfer model based on flow patterns, Int. J. Heat Mass Transfer 51 (1–2) (2008) 125–135.
[22] N. Kattan, J.R. Thome, D. Favrat, Measurement and prediction of two-phase flow patterns for new refrigerants inside horizontal tubes, ASHRAE Trans. 101 (1995) 1251–1257.
[23] N. Kattan, J.R. Thome, D.Favrat, Boiling of R-134a and R-123 in a microfin tube, in: Proc. 19th Int. Congress of Refrigeration, vol. 19, 1996, pp.337–344.
[24] N. Kattan, J.R. Thome, D. Favrat, Flow boiling in horizontal tubes. Part 1: Development of a diabatic two-phase flow pattern map, J. Heat Transfer 120 (1998) 140–147.
[25] N. Kattan, J.R. Thome, D. Favrat, Flow boiling in horizontal tubes. Part 3: Development of a new heat transfer model based on flow patterns, J. Heat Transfer 120 (1998) 156–165.
[26] D. Steiner, Heat transfer to boiling saturated liquids VDI-Wärmeatlas (VDI Heat Atlas), VDI-Gesellschaft Verfahrenstechnik und Chemieingenieurswesen (GCV), Düsseldorf .
[27] Y. Taitel, A. Dukler, A model for predicting flow regime transitions in horizontal and near-horizontal gas-liquid flow, Am. Inst. Chem. Eng. 22 (1976) 47–55.
[28] D. Shao, E. Granryd, Flow pattern, heat transfer and pressure drop in flow condensation. Part I: Pure and azeotropic refrigerants, Int. J. HVAC&R Res. 6 (2000) 175–195.
[29] A. Cavallini, G. Censi, D. Del Col, L. Doretti, G. Longo, L. Rossetto, In-tube condensation of halogenated refrigerants, ASHRAE Trans. 108 (2002) 146–161.
[30] A. Cavallini, D. Del Col, L. Doretti, M. Matkovic, L. Rossetto, C. Zilio, Condensation in horizontal smooth tubes: a new heat transfer model for heat exchanger design, Heat Transfer Eng. 27 (2006) 31–38.
[31] J. El Hajal, J.R. Thome, A. Cavallini, Condensation in horizontal tubes. Part 1: Two-phase flow pattern map, Int. J. Heat Mass Transfer 46 (2003) 3349–3363.
[32] F. Smit, J.R. Thome, J. Meyer, Heat transfer coefficients during condensation of the zeotropic refrigerant mixture HCFC-22/HCFC-142b, J. Heat Transfer 126 (2002) 1137–1146.
[33] A. Lambrechts, L. Liebenberg, A. Bergles, J. Meyer, Heat transfer performance during condensation inside horizontal, smooth micro-fin and herringbone tubes, Journal of Heat Transfer 128 (2006) 691–700.
[34] M. Dobson, J. Chato, Condensation in smooth horizontal tubes, ASME J. Heat Transfer 120 (1998) 193–213.
[35] M. Shah, A general correlation for heat transfer during film condensation inside pipes, Int. J. Heat Mass Transfer 22 (1979) 547–556.

Please cite this article in press as: E. van Rooyen et al., Probabilistic flow pattern-based heat transfer correlation for condensing intermittent flow of refrigerants in smooth horizontal tubes, Int. J. Heat Mass Transfer (2009), doi:10.1016/j.ijheatmasstransfer.2009.12.005

[36] J.R. Thome, J. El Hajal, A. Cavallini, Condensation in horizontal tubes. Part 2: New heat transfer model based on flow regimes, Int. J. Heat Mass Transfer 46 (2003) 3365–3387.
[37] J. Collier, J.R. Thome, Convective Boiling and Condensation, Clarendon Press, Oxford, 1994.
[38] L. Liebenberg, J. Meyer, A review of flow pattern-based predictive correlations during refrigerant condensation in horizontally smooth and enhanced tubes, Heat Transfer Eng. 28 (2008) 12.
[39] K. Cho, S.-J. Tae, Condensation heat transfer for R-22 and R-407C refrigerant-oil mixtures in a microfin tube with a U-bend, Int. J. Heat Mass Transfer 44 (2001) 2043–2051.
[40] M. De Paepe, H. Canière, C. T'Joen, H.-J. Steeman, A. Willockx, M. Christians, E. van Rooyen, L. Liebenberg, J. Meyer, Refrigerant flow regime detection with a capacitance void fraction sensor, AIAA/ASME Joint Thermophys. Heat Transfer Conf. (2006) 1–12.
[41] ASHRAE, Method for measurement of proportion of lubricant in liquid refrigerant, ASHRAE Stand. 41.4 (2006) 1–20.
[42] D. Shao, E. Granryd, Heat transfer and pressure drop of HFC134a-oil mixtures in a horizontal condensing tube, Int. J. Refrig. 18 (8) (1995) 524–533.
[43] L. Liebenberg, J.R. Thome, J. Meyer, Flow visualization and flow pattern identification with power spectral density distributions of pressure traces during refrigerant condensation in smooth and micro-fin tubes, J. Heat Transfer 127 (2005) 209–220.
[44] S. Kline, F. McClintock, Describing uncertainties in single-sample experiments, Mech. Eng. 75 (1953) 3–8.
[45] J. Weisman, D. Duncan, J. Gibson, T. Crawford, Effects of fluid properties and pipe diameter on two-phase flow patterns in horizontal lines, Int. J. Multiphase Flow 5 (1979) 437–462.
[46] REFPROP, NIST thermodynamic properties of refrigerants and refrigerant mixtures (REFPROP), version 8.0, NIST Standard Reference Database 23, National Institute of Standards and Technology 23.
[47] T.A. Partners, Xprops, University of Maryland. Available from: <http://www.thermalanalysispartners.com>.
[48] S. Abu-Eishah, Correlations for the thermal conductivity of metals as a function of temperature, Int. J. Thermophys. 22 (2001) 1855–1868.
[49] T. Tandon, H. Varma, C. Gupta, A new flow regimes map for condensation inside horizontal tubes, J. Heat Transfer 104 (1982) 763–768.
[50] H. Soliman, On the annular-to-wavy flow pattern transition during condensation inside horizontal tubes, Can. J. Chem. Eng. 60 (1982) 475–481.
[51] A. Cavallini, G. Censi, D.D. Col, L. Doretti, G.A. Longo, L. Rossetto, Experimental investigation on condensation heat transfer and pressure drop of new HFC refrigerants (R134a, R125, R32, R410, AR236ea) in a horizontal smooth tube, Int. J. Refrig. 24 (1) (2001) 73–87.

Please cite this article in press as: E. van Rooyen et al., Probabilistic flow pattern-based heat transfer correlation for condensing intermittent flow of refrigerants in smooth horizontal tubes, Int. J. Heat Mass Transfer (2009), doi:10.1016/j.ijheatmasstransfer.2009.12.005